

The Thermochemistry and Reaction Pathways of Energetic Material Decomposition and Combustion

Carl F. Melius

Phil. Trans. R. Soc. Lond. A 1992 **339**, 365-376

doi: 10.1098/rsta.1992.0042

Email alerting service

Receive free email alerts when new articles cite this article - sign up in the box at the top right-hand corner of the article or click [here](#)

To subscribe to *Phil. Trans. R. Soc. Lond. A* go to:
<http://rsta.royalsocietypublishing.org/subscriptions>

The thermochemistry and reaction pathways of energetic material decomposition and combustion

BY CARL F. MELIUS

Combustion Research Facility, Sandia National Laboratories, Livermore, California 94551-0969, U.S.A.

The chemical processes involved in the decomposition and combustion of energetic materials have been investigated theoretically using quantum chemical methods to determine the thermochemistry and reaction pathways. The Bond-Additivity-Corrected Møller–Plesset fourth-order perturbation theory method (BAC-MP4) has been used to determine heats of formation and free energies of reaction intermediates of decomposition and combustion. In addition, the BAC-MP4 method has been used to determine reaction pathways involving these intermediates. A theoretical method for calculating solvation energies has been developed to treat the non-idealities of high pressure and the condensed phase. The resulting chemical processes involving decomposition, ignition and combustion are presented for nitramines and nitromethane. Differences in decomposition mechanisms for the condensed phase and gas phase are discussed. In addition, we discuss the effects that amines can have on the initial stages of condensed-phase nitromethane decomposition. Bond dissociation energies for nitro-triazoles are compared with those of other nitro compounds.

1. Introduction

The decomposition of energetic materials represents a hostile environment of high temperatures and pressures and short timescales. Although it is difficult experimentally to study the molecular processes of decomposition under these conditions, these processes are computationally accessible to theoretical chemistry and detailed chemical kinetics modelling. The ability to model energetic materials requires a knowledge of the thermochemical properties of the initial energetic compound as well as those of the intermediates formed during the decomposition process. From the thermochemical properties one can determine the bond dissociation energies of a molecular compound and its subsequent reaction intermediates. By using these same theoretical chemistry techniques, one can also determine reaction pathways and the activation energies involved in going from reactants to products.

In this paper, we review the application of the BAC-MP4 (Bond-Additivity-Corrected Møller–Plesset fourth-order perturbation theory) quantum chemical procedure (Melius 1990*a*) to investigate dissociation energies of various energetic molecules and decomposition pathways for various energetic materials, including nitromethane and nitramines (Melius 1990*b*). While the BAC-MP4 method provides accurate gas-phase thermochemistry, it does not include the effects of the condensed phase and high-pressure real-gas non-ideality. We therefore present a formalism for

Phil. Trans. R. Soc. Lond. A (1992) **339**, 365–376
Printed in Great Britain

© 1992 The Royal Society and the author

365

treating condensed phase and non-ideal gas effects within the detailed kinetics modelling (Melius *et al.* 1990). We present our current efforts to determine the thermochemistry of the decomposition processes in the condensed phase.

2. Theoretical approach

(a) *Ideal-gas chemical thermodynamics*

The thermochemistry of the reactants, products, and transition state structures were calculated using the BAC-MP4 method (Melius 1990*a*). The geometry optimization and vibrational frequencies were calculated using the Hartree–Fock method with a 6–31G* basis set, whereas the electronic energies were calculated using fourth-order perturbation theory with a 6–31G** basis set. Bond-additivity corrections were applied to the *ab initio* electronic energies. Statistical mechanics methods were applied to the geometries, frequencies and energies to provide heats of formation, entropies and free energies. The details of the BAC-MP4 method with respect to its application to energetic materials have been presented in detail in the reference by Melius (1990*a*).

(b) *Real-gas effects on chemical thermodynamics*

The resulting thermodynamic properties derived from the method discussed above are appropriate for non-interacting molecules in an ideal gas. The stability of decomposition intermediates as well as the reaction mechanisms will be affected by high pressures and condensed phases. We have recently developed a procedure using equations of state whose critical properties can be obtained theoretically from the BAC-MP4 method (Melius *et al.* 1990). The procedure uses transition state theory to treat transition state structures as additional species whose thermodynamic properties can be determined using the same equations of state. By using the thermodynamic formulation of conventional transition state theory, the reaction rate k is given in terms of the Gibbs energy of activation $\Delta G^{\ddagger*}$, i.e.

$$k = (k_b T/h) v^{-\Delta\nu} \exp[-\Delta G^{\ddagger*}/RT]. \quad (2.1)$$

The relation between the real gas partial molar Gibbs energy μ_i , the pure species ideal gas Gibbs energy μ_i^0 (equal to the standard Gibbs energy of formation ΔG_{f298}^0 computed by the BAC-MP4 method), and the partial molar departure function μ_i^D (computed from an equation of state) is given by:

$$\mu_i = \mu_i^0 + RT \ln(P/P^0) + \mu_i^D + RT \ln x_i = G_i^* + RT \ln x_i, \quad (2.2)$$

where x_i is the mole fraction of species i and G_i^* is an effective Gibbs energy for a species in the high-density environment.

To obtain the molecular parameters for the equation of states, i.e. the critical volumes and critical temperatures for transition state structures and other molecular species, we are developing theoretical methods based on the polarizable continuum model for solvents (Miertus *et al.* 1991). The surrounding medium is treated as a continuum dielectric. The method involves several steps. First, we obtain the molecular geometry and electronic wavefunction from the BAC-MP4 calculation. Next, the interface between the molecule and the dielectric continuum of the surrounding medium is defined by the contact surface of the solvent molecule rolling around the scaled van der Waal's surface of the molecule. The boundary-element

method is used to represent the triangulated surface, as developed by Zauhar & Morgan (1990). The volume of the molecule is obtained directly from this boundary-element representation of the molecular surface. Next, the electric potential and the electric field at the surface of the molecule are evaluated from the BAC-MP4 calculation, using the Hartree–Fock 6-31G** basis set wavefunction. The electric potential is used to determine effective atomic charges (using a least-squares fit with constraints for net charge and dipole moments). Applying Gauss' law, the resulting electric field at the molecule surface (obtained from the atomic charges) is used to determine the effective charge of the dielectric continuum at the surface. The surface charge is then used to determine the free energy of hydration. The surface area of the molecule is used to determine the free energy of cavitation (the energy to create a cavity in the dielectric continuum for the molecule). The sum of the free energy of hydration and free energy of cavitation represents the free energy of solvation.

Applications of this solvation method for volumes of activation and activation free energies will be discussed in §3*d* regarding condensed phase decomposition mechanisms for nitromethane. We are currently in the process of implementing the resulting volumes and free energies to determine critical volumes and temperatures for equations of state.

(c) Detailed chemical kinetics modelling

The detailed chemical kinetics modelling of decomposition, ignition and combustion of energetic material involves the simultaneous treatment of convection and diffusive transport of mass, momentum and energy along with the chemical reactions between many molecular species including reactants, intermediates and products. Details of the method can be found in a paper by Melius (1990*b*) and references therein. Lin and co-workers, in collaboration with the author, have been applying this method to elementary reaction rate studies (He *et al.* 1991; Wang *et al.* 1991) as well as to the complex reactions involving the subsequent intermediates of decomposition of energetic materials (Lin *et al.* 1990). The study of the CH₂O/NO₂ system by Lin *et al.* (1990) provides an excellent example of the combination of detailed chemical kinetics modelling and the BAC-MP4 method with experimental shock-tube data. It also provides an example of the use of sensitivity analysis in interpreting the chemical kinetics model. The detailed chemical kinetics modelling has also been applied by the author and co-workers to study combustion flames of the decomposition products of nitramines (Thorne & Melius 1990) and to the combustion of cyclotrimethylene trinitramine (RDX) (Melius 1988, 1990*b*).

3. Applications

(a) Bond energies of nitro groups

The BAC-MP4 method provides an accurate means of obtaining bond dissociation energies (BDES) of energetic materials and reaction intermediates. In this section, we apply this approach to the BDES of nitro compounds. The procedure involves calculating the standard heats of formation at 298 K, ΔH_{f298}° , for the reference molecule as well as for the two radical species formed by breaking the bond. In table 1, we present the bond dissociation energies for selected nitro compounds involving C–NO₂ and N–NO₂ compounds. We find that the R₂N–NO₂ compounds (nitramines) have weaker bond strengths than the R₃C–NO₂ compounds. Also, nitramine (NH₂NO₂), methyl nitramine (CH₃NHNO₂), and dimethylnitramine ((CH₃)₂NNO₂)

Table 1. Calculated bond dissociation energies for various nitro compounds
(BDEs are determined from BAC-MP4 heats of formation at 298 K.)
(energies in kcal mol⁻¹)

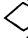
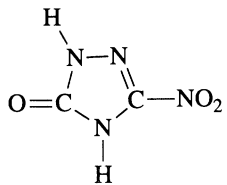
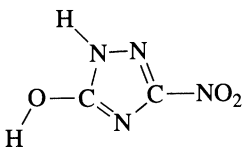
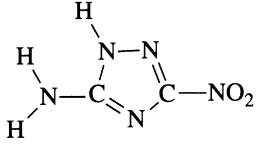
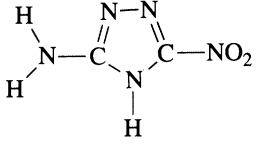
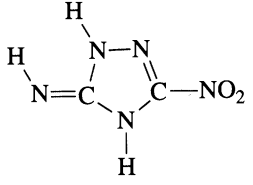
C-nitro compounds		N-nitro compounds	
CH ₃ -NO ₂	58.9	NH ₂ -NO ₂	51.4
C ₂ H ₅ -NO ₂	60.8	CH ₃ NH-NO ₂	50.6
NH ₂ CH ₂ -NO ₂	59.2	(CH ₃) ₂ N-NO ₂	47.2
HN=CH-NO ₂	59.8	 N-NO ₂	50.6
CH ₂ =CH-NO ₂	70.2	CH ₂ =N-NO ₂	37.1
C ₆ H ₅ -NO ₂	72.4		
HOCH=CH-NO ₂	77.0		
NH ₂ CH=CH-NO ₂	78.2		

Table 2. Calculated heats of formation, ΔH_{f298}° , and bond dissociation energies for various 3-nitro-1,2,4-triazole compounds
(energies in kcal mol⁻¹)

compound	ΔH_{f298}°	BDE	compound	ΔH_{f298}°	BDE
	-2.6	71.9		4.0	72.1
	46.6	74.2		52.7	74.6
	60.5	75.6			

have similar N-NO₂ bond dissociation energies (*ca.* 47–51 kcal mol⁻¹), even when strain energy is introduced, such as in N-nitro azetidine. This indicates that group-additivity concepts can be applied to estimating heats of formation of larger nitramine compounds.

For the C-nitro class, neighbouring groups can affect the bond dissociation energy. Replacing a hydrogen atom of nitromethane by a methyl or amino group has little effect on the BDE. Similarly, replacing the hydrogens by an imino (C=N) double bond also has little effect on the BDE. On the other hand, replacing the hydrogens by

† 1 cal \approx 4.184 J.

Table 3. Heats of formation at 298 K, ΔH_{f298}° , and free energies, ΔG_f° , at selected temperatures for the chemical composition $C_1H_3N_1O_2$ ordered by decreasing enthalpy at 298 K (energies in kcal mol⁻¹)

molecular species	ΔH_{f298}°	ΔG_f°		
		300	1000	2000
CH ₃ +NO ₂	42.0	46.6	58.9	77.8
CH ₃ O+NO	28.2	32.5	44.6	63.5
CH ₂ O+HNO	-2.6	1.9	15.1	36.6
CH ₂ N(O)OH	-2.9	13.5	53.4	110.3
HCNO+H ₂ O	-15.0	-8.7	7.0	30.5
CH ₃ ONO	-15.3	0.6	40.4	96.1
$\frac{1}{2}$ CH ₂ O+ $\frac{1}{2}$ CH ₃ OH+NO	-15.9	-11.0	-2.6	23.8
CH ₂ (OH)NO	-16.4	-1.3	35.1	86.8
CH ₃ NO ₂	-16.8	-2.0	34.4	86.6
CH(OH)N(O)H	-30.1	-13.7	26.9	84.6
CH(OH)NOH	-45.3	-29.4	9.5	64.6
CH(O)NHOH	-45.7	-29.8	9.2	64.4
CO+H ₂ O+ $\frac{1}{2}$ N ₂ + $\frac{1}{2}$ H ₂	-84.2	-87.4	-94.1	-101.1
HNCO+H ₂ O	-86.4	-81.0	-67.2	-45.4
C(OH) ₂ NH	-87.3	-71.0	-31.4	24.8
CO ₂ + $\frac{1}{2}$ N ₂ + $\frac{3}{2}$ H ₂	-94.1	-94.3	-94.8	-95.2
CO ₂ +NH ₃	-105.1	-98.2	-80.0	-52.2
C(NH ₂)(O)OH	-106.2	-90.3	-51.7	2.9

a C=C double bond increases the BDE by *ca.* 10 kcal mol⁻¹. Replacing the β -carbon hydrogen by a hydroxyl or amino group adds an additional *ca.* 7–8 kcal mol⁻¹. The BDE for nitrobenzene is similar to nitroethylene, both having a C=C double bond adjacent to the C-nitro bond.

In table 2, we present the heats of formation at 298 K, ΔH_{f298}° , as well as the BDEs for 3-nitro-1,2,4-triazole compounds, including tautomers of 3-nitro-1,2,4-triazole-5-one (NTO) and 3-nitro-5-amino-1,2,4-triazole. Although the heats of formation of the tautomers differ, the tautomers have similar BDEs. The 3-nitro-1,2,4-triazole's have an increased BDE of *ca.* 13 kcal mol⁻¹ compared with HN=CHNO₂, which also has a neighbouring imino bond. The increase in bond strength is comparable with the increase in the C–NO₂ bond energy due to a neighbouring C=C double bond. Thus, the 1,2,4-triazole ring provides stabilization of the nitro bond. Plots of the electric field on the surface of the molecule indicates increased positive charge in the C-nitro bond of NTO compared with nitromethane ($q_C = +0.35$ for NTO against $q_C = -0.22$ for CH₃NO₂). The enhanced ionic character of NTO provides greater stabilization of the compound in the condensed phase.

(b) *Chemistry of gas-phase nitromethane decomposition and ignition*

The detailed chemical kinetics modelling approach has been used to study the chemistry of nitromethane ignition and detonation (Melius 1990*b*). Temperature, pressure, and species profiles as a function of time for atmospheric ignition of gaseous CH₃NO₂ and shock initiated detonation of gaseous CH₃NO₂ have been given in the reference by Melius (1990*b*). The overall reaction chemistry of the first stage ignition is primarily



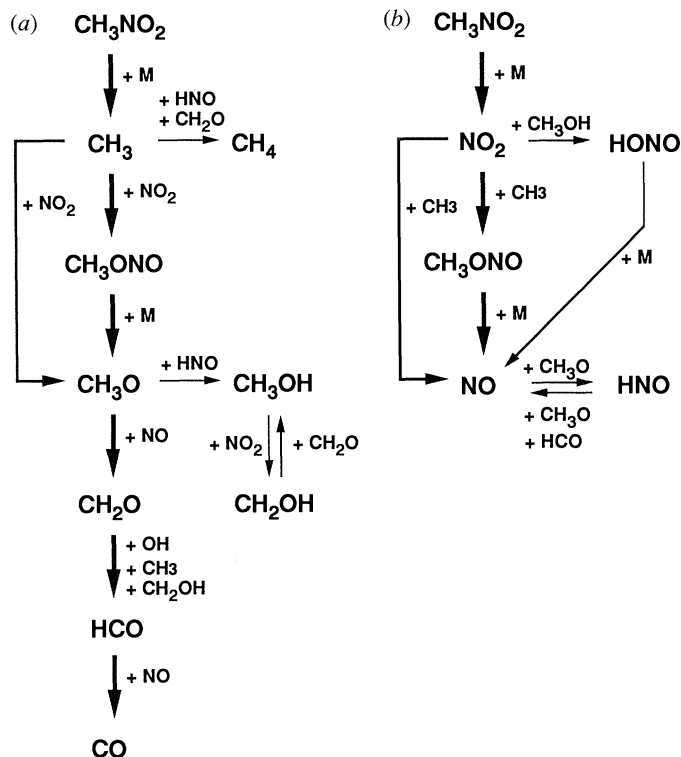
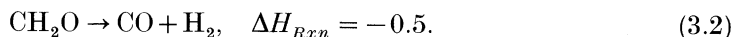


Figure 1. Reaction mechanism diagrams for (a) carbon-containing and (b) nitrogen-containing species during the first stage ignition of nitromethane. Unimolecular decomposition is indicated by the third-body notation +M. Thick arrows indicate major reaction pathways.

with the later conversion of formaldehyde to carbon monoxide



The reactions are essentially thermoneutral, yielding very little temperature rise. The increase in pressure arises from the conversion of one mole of nitromethane into two moles of intermediates. The overall reaction, which reduces the free energy, is driven by the increase in entropy of phase space resulting from the increase in the number of molecules formed. This can be seen in table 3, where we list heats of formation and free energies for chemical species with a net composition corresponding to that of nitromethane ($\text{C}_1\text{H}_3\text{N}_1\text{O}_2$). Mixing terms, not included in table 3, contribute further to the increase in entropy. The majority of heat release in nitromethane occurs in the second stage ignition which converts NO to N_2 . A reaction flow diagram for the first stage ignition is given in figure 1. In nitromethane, the conversion of CH_3O to CH_3OH and CH_2O provides the sources of heat for the first ignition stage, after which CH_3OH is converted back to CH_2O and then to CO during the first stage ignition.

(c) Chemical reaction mechanisms of an RDX flame

The nitromethane ignition considered above is a zero-dimensional, well-mixed problem, depending only on time. As a more complicated system, we summarize results for modelling of a steady-state RDX flame (Melius 1988, 1990b). The flame model is one-dimensional, including mass and species diffusion as well as detailed

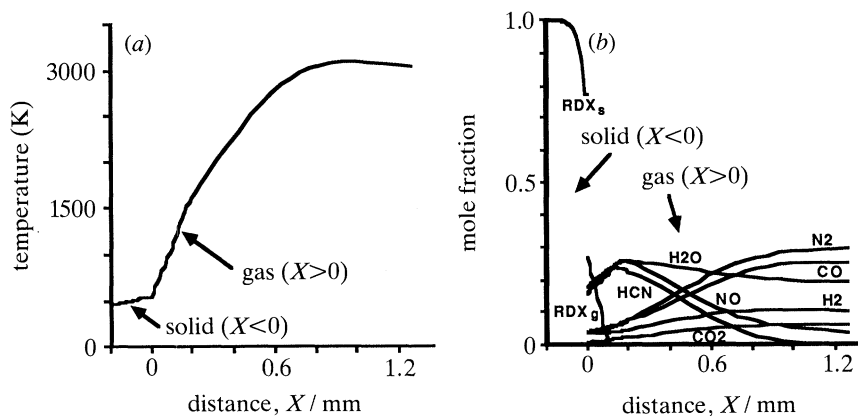


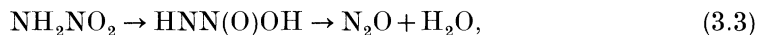
Figure 2. Temperature (a) and species concentration (b) (mole fraction) profiles as a function of distance (mm) for an RDX flame at 1 atm. Origin corresponds to the gas-solid interface.

chemical kinetics. The resulting temperature and species profiles as a function of distance above the surface of the propellant for a 1 atm† flame are given in figure 2. In figure 3, we present the chemical reaction flow diagrams for the RDX flame. Separate reaction chemistry pathways are indicated for the carbon species, the nitrogen species of the amino group of the RDX ring, and the nitrogen chemistry of nitro group of RDX. The results indicate a two-stage flame chemistry. The OH radical dominates the primary zone chemistry. The thermal decomposition of HONO provides the source of OH radicals in the primary flame. HONO plays an analogous role to CH_3OH in nitromethane by providing a temporary source of heat for the first stage ignition. Unimolecular decomposition of N_2O provides the radical source to drive the second stage chemistry.

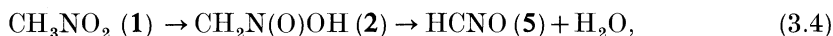
(d) *Condensed phase effects on thermochemistry and reaction mechanisms*

In both the gas-phase nitromethane ignition and the gas-phase RDX flame, the chemistry is dominated by radicals, arising from unimolecular bond fissioning (see figures 1 and 3). In the condensed phase, the temperatures are lower, precluding significant formation of radicals. For example, HONO elimination occurs rather than NO_2 bond fissioning. Though the mechanism changes, we find that the BAC-MP4 derived activation energies and heats of reaction for the HONO elimination for various classes of nitro compounds correlate with the bond dissociation energies (Melius 1990a).

Besides unimolecular rearrangement, solvent stabilization effects as well as catalytic effects of the condensed phase provide concerted reaction pathways. During the initial stages of decomposition in the condensed phase, the formation of water can autocatalyse the decomposition process. As an example, the presence of water provides a concerted, cyclic reaction pathway for reduction of the nitro group (Melius 1990a). In figure 4, we show the reaction pathways for decomposition of nitramine,



and nitromethane,



† 1 atm $\approx 10^5$ Pa.

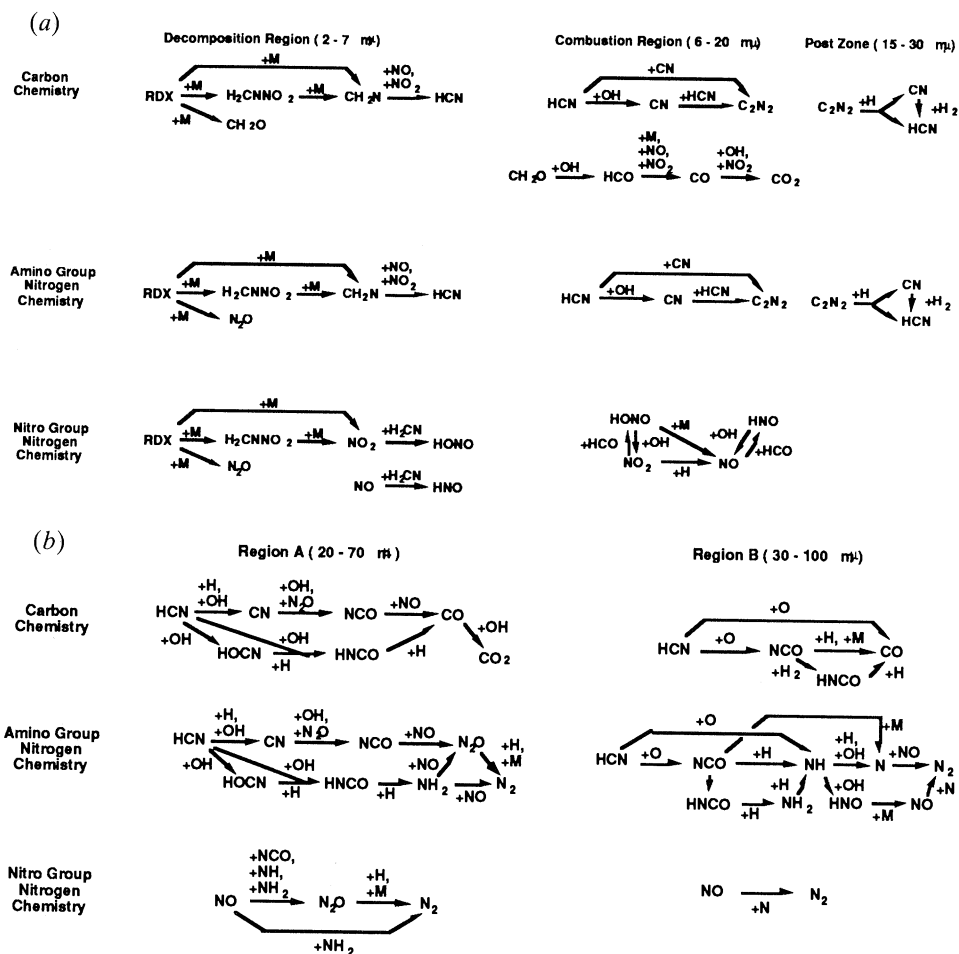


Figure 3. Chemical reaction flow diagrams for the (a) primary and (b) secondary stages of an RDX flame at 17 atm. The spatial extent of each region is given in micrometres.

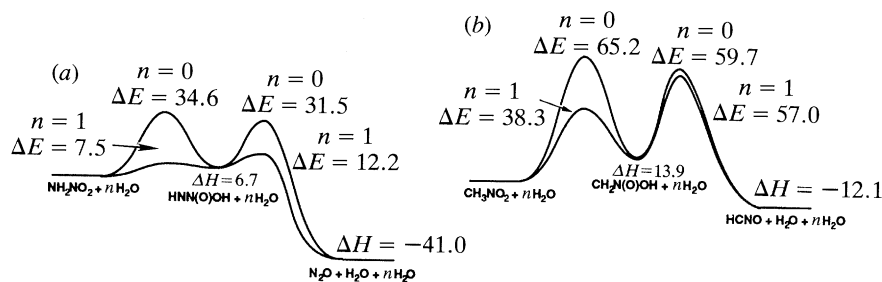


Figure 4. Reaction pathways for the concerted decomposition of (a) nitramine and (b) nitromethane (energies in kcal mol⁻¹).

with and without the presence of water. The $n = 0$ pathway corresponds to a unimolecular four-centred process. The $n = 1$ pathway corresponds to a six-centred bimolecular process involving another water molecule. The transition state structures for the conversion of (1) to the intermediate aci form (2) are shown in figure 5. We

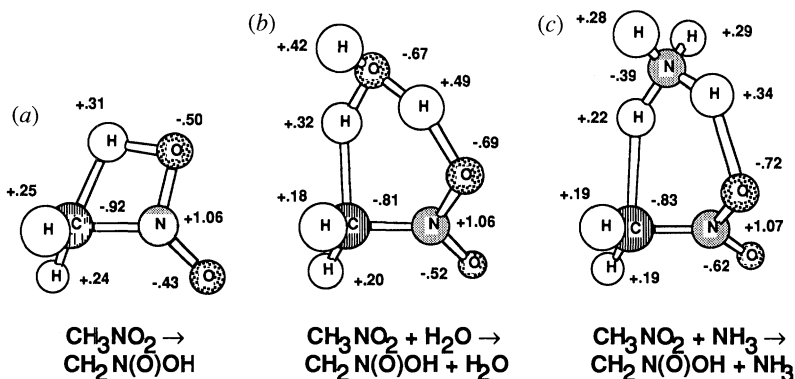


Figure 5. Transition state structures and atomic charges for the conversion of nitromethane, CH_3NO_2 , to the *aci* form, $\text{CH}_2\text{N}(\text{O})\text{OH}$: (a) unimolecular, (b) concerted bimolecular with C_2O , (c) concerted bimolecular with NH_3 .

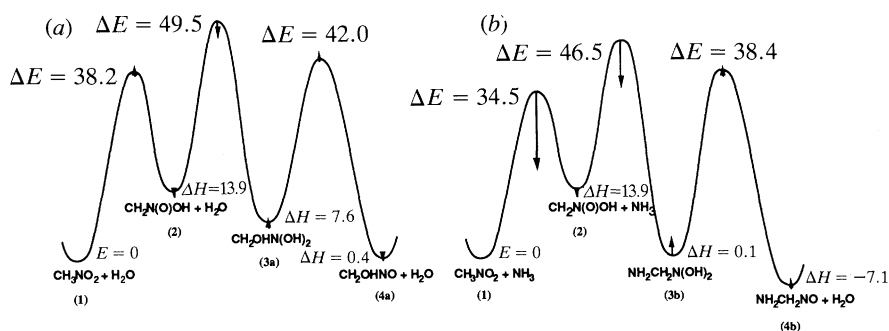
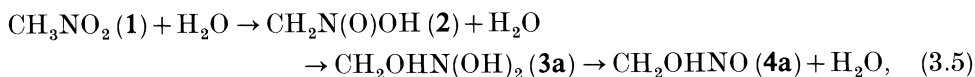


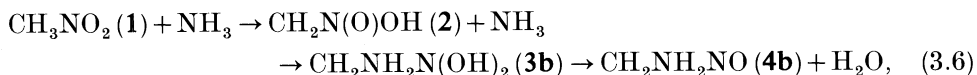
Figure 6. Reaction pathways for the concerted decomposition of CH_3NO_2 to nitroso intermediates due to concerted reactions with (a) water and (b) ammonia. Arrows indicate the extent and sign of the free energy of solvation (energies in kcal mol^{-1}).

see that the barrier for nitramine decomposition is less than that for nitromethane. Furthermore, the catalytic effect of water is dramatic for nitramine. For nitromethane, the catalytic effect of water in reducing the barrier for conversion to the *aci* form (2) is significant but has little effect on further conversion to HCNO .

The addition of amines have been shown to sensitize the decomposition of nitromethane, possibly through the *aci*-ion intermediate (Engelke 1980; Engelke *et al.* 1986). We have carried out BAC-MP4 calculations of the reaction pathways for the initial decomposition of nitromethane, involving the conversion of nitromethane, through the neutral intermediate *aci* form (2), to the nitroso intermediates (4a and 4b).



and



The resulting reaction pathways are shown in figure 6, for water as the catalyst and for ammonia as the catalyst. The transition state structures are shown in figure 5 for

Table 4. Solvation properties of reactants, intermediates, and transition state structures (TS) of decomposition of nitromethane

(1 Å = 10⁻¹⁰ m = 10⁻¹ nm)

molecular structure	ΔG_{sol} (kcal mol ⁻¹)	$V/\text{\AA}^3$	q_{C}	q_{N}
(1) CH ₃ NO ₂	-2.4	51.0	-0.22 (-0.19)	+0.92 (+0.55)
(2) CH ₂ N(O)OH	-4.0	51.0	-0.50 (-0.12)	+0.84 (+0.44)
(3a) HOCH ₂ N(OH) ₂	-6.6	66.2	+0.62 (+0.25)	-0.08 (+0.08)
(3b) NH ₂ CH ₂ N(OH) ₂	-0.2	70.3	+0.79 (+0.15)	-0.20 (+0.03)
(4a) HOCH ₂ NO	-2.6	51.7	+1.14 (+0.24)	-0.21 (+0.04)
(4b) NH ₂ CH ₂ NO	+1.3	56.7	+1.04 (+0.08)	-0.22 (+0.05)
TS (1) → (2)	+2.2	50.6	-0.92 (-0.43)	+1.06 (+0.57)
TS (1) → (2) _{H₂O}	-5.8	66.0	-0.81 (-0.46)	+1.06 (+0.57)
TS (1) → (2) _{NH₃}	-20.5	71.9	-0.83 (-0.40)	+1.07 (+0.55)
TS (2) → (3a) _{H₂O}	-13.5	71.6	+0.12 (+0.19)	+0.08 (+0.14)
TS (2) → (3b) _{NH₃}	-10.7	66.4	+0.31 (+0.22)	0 (+0.10)
TS (3a) → (4a) _{H₂O}	-3.2	70.9	+0.87 (+0.15)	-0.15 (+0.09)
TS (3b) → (4b) _{NH₃}	-5.2	65.6	+0.83 (+0.85)	-0.18 (+0.06)
(5) HCNO	-3.0	37.4	-0.46 (+0.07)	+0.61 (+0.21)
TS (2) → (5)	-6.5	52.8	-0.40 (-0.12)	+0.71 (+0.46)
TS (2) → (5) _{H₂O}	-8.4	68.4	-0.43 (-0.12)	+0.70 (+0.47)
TS (2) → (5) _{NH₃}	-9.5	73.3	-0.69 (-0.22)	+0.82 (+0.36)
NH ₃	-1.5	23.6	—	-1.05 (-0.79)
H ₂ O	-4.4	16.7	—	—

the first step forming (2). The mechanism involves acid/base catalysed proton transfer. The role of the ionic form of these intermediates, such as the aci-ion for (2), may dominate in solution, depending on equilibrium constants. For instance, the transition state structure for (2) + NH₃ → (3b) is for the formation the zwitterionic CH₂(NH₃⁺)N(OH)O⁻ structure, although the zwitterionic structure is not stable with respect to (3b) without solvent stabilization. Furthermore, the water and ammonia catalysed transition state structures for (1) → (2) possess ionic character involving the aci-ion (e.g. in figure 5, the ammonia-catalysed transition state structure possesses significant NH₄⁺-CH₂NO₂- character).

To estimate the effects of solvation stabilization, we have applied the polarizable continuum model discussed in §2b to reactions (3.4), (3.5) and (3.6), using water at 298 K as the solvent. The results are given in table 4 for each molecular structure. For each species, the solvation free energy, ΔG_{sol} , the volume of the molecular structure, V , and the effective atomic charges of the carbon atom, q_{C} , and the nitrogen, q_{N} , are given. For comparison, Mulliken population analysis atomic charges are given in parentheses. The notation TS represents a transition-state structure. The subscript on transition states corresponds to the cyclic transition state involving an additional H₂O or NH₃. In table 5, we give the resulting solvation energies of reaction and activation, ΔG_{sol} , and volumes of reaction and activation, ΔV , for reactions (3.4), (3.5) and (3.6). The column heading H₂O or NH₃ corresponds to a cyclic transition state involving an additional H₂O (3.5) or NH₃ (3.6); X represents OH or NH₂ respectively. These solvation free energies, ΔG_{sol} , are indicated by arrows in figure 6. We see from the ΔV values of table 5 that increasing pressures favour reactions (3.5) and (3.6) over (3.4). The solvation effect of water is rather small for

Table 5. Solvation energies of reaction and activation and volumes of reaction and activation for decomposition pathways of nitromethane

molecular structure	$\Delta G_{\text{sol}}/(\text{kcal mol}^{-1})$			$\Delta V/\text{\AA}^3$		
	—	H ₂ O	NH ₃	—	H ₂ O	NH ₃
(1) CH ₃ NO ₂	0	0	0	0	0	0
TS (1) → (2)	+4.6	+1.0	-16.4	-0.4	-1.7	-2.7
(2) CH ₂ N(O)OH	-1.6	-1.6	-1.6	0.0	0.0	0.0
TS (2) → (3)	—	-3.9	-9.6	—	-1.3	-3.0
(3a, 3b) XCH ₂ N(OH) ₂	—	+0.2	+3.7	—	-1.5	-4.3
TS (3) → (4)	—	+1.6	+0.7	—	-2.1	-3.7
(4a, 4b) XCH ₂ NO	-0.2	-0.2	+0.8	+0.7	+0.7	-1.2
TS (2) → (5)	-4.1	-1.6	-5.6	+1.8	+0.7	-1.3
(5) HNCO + H ₂ O	-5.0	-5.0	-5.0	+3.1	+3.1	+3.1

reaction (3.5) compared with the catalytic effect. (Stabilization of ionic species, such as the aci-ion and zwitterions mentioned above, on the other hand, is expected to be large.) Meanwhile, solvation stabilization exhibits large effects on the ammonia catalysed reaction (3.6), particularly in the reaction rate for formation of the aci-form (2) of nitromethane. Finally, we point out that the amino adducts (3b) and (4b) are more stable than their hydroxy counterparts (3a) and (4a), enhancing the role of amines in the reduction chemistry of converting nitromethane through the nitroso intermediates to N₂O. These results provide theoretical support to the general observations of Engelke *et al.* (1986) on the correlation of the aci-ion in amine sensitization of nitromethane.

Finally, note that Cook & Haskins (1989 and references therein) have considered an alternative C-nitro bond-breaking initial step in amine sensitization of nitromethane. The solvent stabilization effects addressed here should help stabilize their mechanism, though it is uncertain whether it can compete with the amine addition to the aci-form (2) in (3.6). It is necessary to convert the negatively charged carbon moiety to a positively charged carbon moiety (see table 4) as part of the base-catalysed hydration and hydrolysis of nitromethane to more stable products.

4. Conclusions

The BAC-MP4 quantum chemistry method and detailed kinetics modelling has been used to investigate the decomposition mechanism of energetic materials at the molecular level. Thermochemical properties of intermediate species and transition state structures are used to determine initial bond breaking in energetic molecules. Chemical kinetics modelling using these results provide reaction pathways by which decomposition and oxidation occur during ignition and deflagration. Catalytic effects and solvation effects of the condensed phase alter these reaction pathways.

The author acknowledges the contributions of all the collaborators, including Dr N. Bergan, Dr J. S. Binkley, Dr M. C. Lin, Dr J. A. Miller, Dr S. Odier, Dr J. E. Shepherd, and Dr L. R. Thorne, who have contributed to the various parts of this research. The author would also like to acknowledge the programmatic and funding stimulus of Dr R. S. Miller of the Office of Naval Research in making this work possible.

This work was supported by the Department of Energy and by the Office of Naval Research (N00014-90-F-0078).

References

- Cook, M. D. & Haskins, P. J. 1989 Decomposition mechanisms and chemical sensitization in nitro, nitramine, and nitrate explosives. In *Proc. Ninth symp. (Int.) on Detonation*, pp. 1027–1030. Portland, Oregon.
- Engelke, R. 1980 Effect of a chemical inhomogeneity on steady-state detonation velocity. *Phys. Fluids* **23**, 875–880.
- Engelke, R., Earl, W. L. & Rohlfling, C. M. 1986 Production of the nitromethane aci-ion by UV irradiation: its effect on detonation sensitivity. *J. phys. Chem.* **90**, 545–547.
- He, Y., Liu, X., Lin, M. C. & Melius, C. F. 1991 The thermal reaction of HNCO at moderate temperatures. *Int. J. chem. Kinetics* **23**, 1129.
- Lin, C.-Y., Wang, H.-T., Lin, M. C. & Melius, C. F. 1990 A shock tube study of the $\text{CH}_2\text{O} + \text{NO}_2$ reaction at high temperatures. *Int. J. chem. Kinetics* **22**, 455–482.
- Melius, C. F. 1988 The gas-phase flame chemistry of nitramine combustion. In *Proc. 25th JANNAF Combustion Meeting*, vol. II, pp. 155–162.
- Melius, C. F. 1990a Thermochemical modelling: I. Application to decomposition of energetic materials. In *Chemistry and physics of energetic materials* (ed. S. Bulusu), ASI **309**. NATO.
- Melius, C. F. 1990b Thermochemical modelling: II. Application to ignition and combustion of energetic materials. In *Chemistry and physics of energetic materials* (ed. S. Bulusu), pp. 51–78, ASI **309**. NATO.
- Melius, C. F., Bergan, N. & Shepherd, J. E. 1990 Effects of water on combustion kinetics at high pressure. In *Proc. 23rd Symp. (Int.) on Combustion*, pp. 217–223. Pittsburgh: the Combustion Institute.
- Miertus, S., Scrocco, E. & Tomasi, J. 1981 Electrostatic interactions of a solute with a continuum. A direct utilization of *ab initio* molecular potentials for the provision of solvent effects. *Chem. Phys.* **99**, 77–82.
- Thorne, L. R. & Melius, C. F. 1990 The structure of hydrogen cyanide-nitrogen dioxide premixed flames. In *Proc. 23rd Symp. (Int.) on Combustion*, pp. 397–403. Pittsburgh: The Combustion Institute.
- Wang, N. S., Yang, D. L., Lin, M. C. & Melius, C. F. 1991 Kinetics of CN reactions with N_2O and CO_2 . *Int. J. chem. Kinetics* **23**, 151–160.
- Zauhar, R. J. & Morgan, R. S. 1990 The rigorous computation of the molecular electric potential. *J. Comp. Chem.* **9**, 171–187.